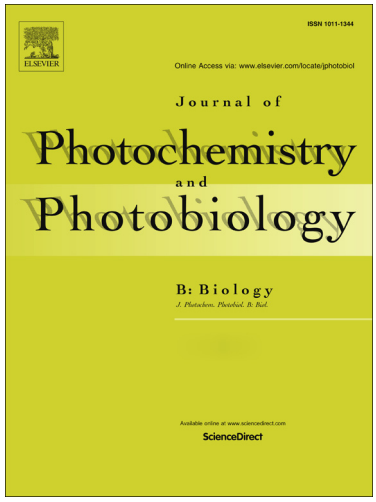

Interaction between Human Serum Albumin and antidiabetic compounds and its influence on the $O_2(^1\Delta_g)$-mediated degradation of the protein

C. Challier, P. Beassoni, C. Boetsch, N.A. Garcia, M.A. Biasutti, S. Criado

PII: S1011-1344(14)00327-3
DOI: http://dx.doi.org/10.1016/j.jphotobiol.2014.10.019
Reference: JPB 9871

To appear in: *Journal of Photochemistry and Photobiology B: Biology*

Received Date: 14 August 2014
Revised Date: 28 October 2014
Accepted Date: 30 October 2014

Please cite this article as: C. Challier, P. Beassoni, C. Boetsch, N.A. Garcia, M.A. Biasutti, S. Criado, Interaction between Human Serum Albumin and antidiabetic compounds and its influence on the $O_2(^1\Delta_g)$-mediated degradation of the protein, *Journal of Photochemistry and Photobiology B: Biology* (2014), doi: http://dx.doi.org/10.1016/j.jphotobiol.2014.10.019

Interaction between Human Serum Albumin and antidiabetic compounds and its influence on the $O_2(^1\Delta_g)$-mediated degradation of the protein

C. Challier[a*], P. Beassoni[b], C. Boetsch[b], N. A. Garcia[a], M. A. Biasutti[a] and S. Criado[a*]

[a] Departamento de Química, Universidad Nacional de Río Cuarto, X5804BYA Córdoba, Argentina.

[b] Departamento de Biología Molecular, Universidad Nacional de Río Cuarto, X5804BYA, Córdoba, Argentina

*Corresponding authors: Susana Criado, Tel/FAX.: +54 358 467 6233, e-mail: scriado@exa.unrc.edu.ar. Cecilia Challier, Tel./FAX: +54 358 467 6233, e-mail: cchallier@exa.unrc.edu.ar.

ABSTRACT

The complexity depicted by disease scenarios as diabetes *mellitus*, constitutes a very interesting field of study when drugs and biologically relevant components may be affected by such environments. In this report, the interaction between the protein Human Serum Albumin (HSA) and two antidiabetics (Andb), Gliclazide (Gli) and Glipizide (Glip) was studied through fluorescence and docking assays, in order to characterize these systems. On the basis that HSA and Andb can be exposed *in vivo* at high Reactive Oxygen Species (ROS) concentrations in diabetic patients, the degradative process of the protein free and bound to Andb, in presence of the species singlet molecular oxygen ($O_2(^1\Delta_g)$), was evaluated. Fluorescence and docking assays indicated that Gli, as well as Glip bind to HSA on two sites, with binding constants values in the order of 10^4-10^5 M^{-1}. Likewise, docking assays revealed that the location of Gli or Glip on the protein may be the HSA binding sites II and III. Thermodynamic parameters showed that the interaction between HSA and Glip is a favored, enthalpically-controlled process. Oxygen uptake experiments indicated that Glip is less photooxidizable than Gli through a $O_2(^1\Delta_g)$-mediated process. Besides, the protein-Andb binding produced a decrease in the overall rate constant for $O_2(^1\Delta_g)$ quenching as compared to the value for the free protein. This fact could be interpreted in terms of a reduction in the availability of Tyrosine residues in the bonded protein, with a concomitant decrease in the physical quenching deactivation of the oxidative species.

Keywords: binding, docking, photodegradation, Gliclazide, Glipizide, oxidative stress, human serum albumin.

Abbreviations

HSA: Human Serum albumin

Andb: Antidiabetics

Gli: Gliclazide

Glip: Glipizide

ROS: Reactive Oxygen Species

$O_2(^1\Delta_g)$: singlet molecular oxygen

PN: Perinaphtenone

TRPD: Time-resolved phosphorescence detection of O_2 ($^1\Delta_g$)

rmsd: root mean square deviation

Trp: tryptophan

K_{bi}: association or binding constant

r: binding density

n: total number of binding sites

θ: fractional occupancy

R: universal gas constant

Tyr: Tyrosine

Glu: Glutamic acid

Phe: Phenylalanine

Ala: Alanine

Ser: Serine

Lys: Lysine

Gln: Glutamine

Arg: Arginine

Leu: Leucine

His: Histidine

Ile: Isoleucine

Asn: Asparagine

Val: Valine

Pro: Proline

Met: Methionine

S: sensitizer

A: photooxidable substrate

1. INTRODUCTION

Protein binding describes the ability of biomolecules to interact with other species through reversible or irreversible processes. In fact, the biological properties of a protein are highly dependent on its binding abilities. In this sense, enzymatic action, hormone activity and genic regulation are some examples of important biological processes wherein protein binding plays very important roles [1]. Drug transport is another example of such processes, in which the binding of drugs to serum proteins has an important effect on their distribution and therapeutic action, since only free drugs are able to interact with their specific receptor [2].

In humans, the most abundant of serum proteins is Human Serum Albumin (HSA) and its main function is the transport of compounds. Besides, this protein presents enzymatic activities as well as important antioxidant functions in blood serum [3]. Thus, HSA is a multifunctional protein, and most of its properties are principally derived from its ligand-binding abilities. In this context, it is well known that under disease scenarios such as cancer, diabetes *mellitus*, and liver o renal pathology, these protein binding properties can be seriously altered [2].

Particularly, diabetes *mellitus* is a group of metabolic diseases characterized by hyperglycemia resulting from defects in insulin secretion, insulin action or both [4]. The characteristic high blood glucose concentrations associated with this disease generate a cascade of processes which may affect, among many other, protein binding functions [5]. Diabetes *mellitus* is a world widely disseminated disease that has increased very fast along the last years. In fact, around 8 % of the total world population suffers this disease and it is

estimated that the number of patients will rise even more in future years [4]. The vast majority of cases of diabetes fall into two broad ethiopatogenic categories: diabetes *mellitus* type I, and the more prevalent diabetes *mellitus* type II (around 80% of the patients). At present, the treatment for diabetes type II includes the use of the second-generation sulfonylurea compounds such as Gliclazide, Glipizide, Glibenclamide and Glimepiride. These antidiabetics (Andb), considered as weak acidic compounds, act by stimulating insulin secretion from beta cells in pancreas and could bind HSA since it is well known that acidic and neutral compounds tend to bind albumin [6,7].

On the other hand, it is well established that elevated sugar levels in diabetic patients is associated with increased Reactive Oxygen Species (ROS) intracellular production, which generates an oxidative stressing environment [8]. In parallel, previous reports demonstrate that oxidative damage plays an important role in diabetes genesis and its complications [5,9-11].

In this context, since Andb and HSA may be exposed to oxidative stress in common microenvironments, the study of the potential effect of ROS on the free and bonded species constitutes an approach of highly practical interest.

In the present contribution, the binding parameters between HSA and Andb were determined through fluorescence measurements and supported with docking assays. Furthermore, the oxidability of free and bonded entities was evaluated employing photogenerated singlet molecular oxygen ($O_2(^1\Delta_g)$) as an archetypal oxidative species in a potential oxidative stressing scenery.

2. MATERIALS AND METHODS

2.1. Materials

Gliclazide (Gli), Glipizide (Glip), Human Serum Albumin (HSA; fatty acid free), Perinaphtenone (PN), deuterated water (99.9 %) and NaOH were obtained from Sigma-Aldrich Argentina S.A. KH_2PO_4 and methanol (HPLC quality) were obtained from Cicarelli and Sintorgan, respectively.

Due to low Andb solubility in aqueous solutions, the experiments were made using methanol as a co-solvent (10%) and 0.1 M phosphate buffer (pH 7.4). The presence of this percentage of methanol does not produce changes in HSA properties [12]. HSA solutions were prepared, based on a molecular weight of 66500Da [13].

2.2. Methods

2.2.1. Determination of binding parameters

HSA is a single chain protein that contains one tryptophan residue (Trp214). Since the emission of this aminoacid is very sensitive to changes in its microenvironment, its fluorescence can be used as a signal for monitoring interactions [14]. So, in binding assays the fluorescence intensities of HSA were determined by monitoring the changes in fluorescence intensities from Trp214.

The binding parameters, association constant (K_{bi}) and total number of binding sites (n), were determined from fluorescence experimental data, using a model of binding isotherm based on the following equation [15].

$$< r >= \sum_{i=1}^{i=n} \frac{K_{bi}[Andb]_{free}}{(1+K_{bi}[Andb]_{free})} \qquad (1)$$

where <r> is the binding density and $[Andb]_{free}$, the molar concentration of Andb unbound to HSA, which can be calculated [16] from Eq. 2

$$[Andb]_{free} = [Andb]_{total} - [Andb]_{bound} \quad (2)$$

$$[Andb]_{bound} = n\theta\,[HSA]_{total} \quad (3)$$

$[Andb]_{total}$ is the total quantity of Andb added and $[Andb]_{bound}$, the amount of drug bound to HSA. The variable θ is the fractional occupancy of the total binding sites in HSA and was obtained from the ratio [17], $\theta = \Delta I/\Delta I_{Max}$ where $\Delta I = I_0 - I$. I_0 and I are the fluorescence intensities of HSA in absence and in presence of Andb, respectively. ΔI_{Max} is the limiting fluorescence difference value approached at high Andb concentrations, obtained from the double reciprocal ($1/\Delta I$ *vs.* $1/[Andb]_{total}$) plots. Finally, in Eq. 3 a given value of n was supposed in order to calculate $[Andb]_{bound}$. Through these values, $[Andb]_{free}$ can be determined (Eq. 2).

On the other hand, the binding density (<r>) was calculated from the relationship:

$$<r> = [Andb]_{bound}/[HSA]_{total} \quad (4)$$

A graphical representation of <r>*vs.* $[Andb]_{free}$ was constructed. Then, the experimental data <r>*vs.* $[Andb]_{free}$ were fitted to Eq. 1, through an iterative nonlinear least squares regression program [18]. It is important to notice that the number of terms used in Eq. 1 must be equal to the n value supposed in the calculation of $[Andb]_{bound}$ (Eq. 3). The same procedure was done trying out different n values in calculation of $[Andb]_{bound}$. The true n value is the one that produces the lowest error in the isotherm fitting. Finally, through this fitting the K_{bi} is calculated.

Fluorescence emission spectra were measured by using Spex Fluoromax equipment. Quartz cuvettes of 1.0 cm of path length were used. Samples were excited at 295 nm and the fluorescence emission was recorded at 340 nm.

The absorption spectra were measured employing Hewlett Packard 8452A diode array spectrophotometer.

On the other hand, thermodynamic parameters for HSA-Andb interaction were determined from binding experiments carried out at four temperatures. Considering that enthalpy change (ΔH^0) does not vary significantly over the temperature range used, ΔH^0 and ΔS^0 were determined using the Van`t Hoff equation:

$$\ln K_{bi} = -\frac{\Delta H^0}{RT} + \frac{\Delta S^0}{R} \qquad (5)$$

where K_{bi} is the binding constant at the corresponding temperature and R is the universal gas constant. The free energy of binding (ΔG^0) was estimated from ΔH^0 and ΔS^0 values using the following relationship:

$$\Delta G^0 = \Delta H^0 - T\Delta S^0 \qquad (6)$$

2.2.2. Docking assays

The docking studies were carried out as previously described [19]. Briefly, ICM version 3.4 was used and the icmPocketFinder function was employed to detect possible binding sites with a tolerance of 4.6 by default [20]. This parameter is related to flexibility for sites prediction. The lower the tolerance value the more pockets predicted and the higher the tolerance the

less pockets predicted. We used the value recommended by software developers; the tool was accurate to predict sites coincident with crystallographic location of several drugs in the PDB structures analyzed. Ligand inputs were extracted from the PubChem data base [21]. All structures were protonated and optimized using standard ICM protocols. The thoroughness parameter, which represents the length of the docking simulation was set at 1.0, as recommended by software developers.

A search of molecules of HSA co-crystallized with different ligands was performed in the Protein Data Bank (http://www.rcsb.org/) and all the molecules analyzed in this work were the following: 1AO6, 1E7C, 1GNI, 1HK3, 1UOR, 2BXD, 2BXK, 2BXQ,1BJ5, 1E7E, 1GNJ, 1HK4, 1YSX, 2BXE, 2BXL, 1BKE, 1E7F, 1H9Z, 1HK5, 2BX8, 2BXF, 2BXM, 1BM0, 1E7G, 1HA2, 1N5U, 2BXA, 2BXG, 2BXN, 1E7A, 1E7H, 1HK1, 1O9X, 2BXB, 2BXH, 2BXO,1E7B, 1E7I, 1HK2, 1TF0, 2BXC, 2BXI and 2BXP. Docking assays were performed mapping the so called “Sudlow” binding sites (Sites I and II) and the binding site III [22].

HSA complexed with warfarin (PDB:2BXD) was used as receptor molecule. The method was validated by docking of warfarin, diazepam and azapropazone in binding sites I, II and III of this protein, respectively. For this, the ligands were docked, expecting to reproduce the experimentally determined positions. For docking in site I, the gridbox size was 21.5 Å x 27.5 Å x 22.5 Å and the center was located at the points (4.43, -9.00, 7.02) Å. For docking in site II, the gridbox size was 21.5 Å x 20.0 Å x 16.5 Å and the center was located at the points (7.79, 2.64, -15.45) Å. For docking in site III, the gridbox size was 24.5 Å x 27.5 Å x 33.0 Å and the center was located at the points (-1.28, 8.75, 5.86) Å.

2.2.3. Sensitized photoirradiation of Andb and HSA

2.2.3.1. Stationary photolysis

Stationary aerobic photolysis of aqueous buffered solutions at pH 7.4 (10% methanol) containing Andb (0.5 mM) and the sensitizer PN (A_{365nm} = 0.5) were carried out in a home-made photolyser [23]. It is provided with a quartz-halogen lamp (OSRAM XENOPHOT HPLX 64640, 150w-24 V G35, OSRAM Augsburg, Germany). The light was passed through a water filter and focused on a hermetically sealed reaction cell with a specific oxygen electrode (Orion 97-08). The solutions were continuously stirred. Light at λ< 320 nm was filtered using a cut-off filter in order to ensure that the light was only absorbed by the sensitizer. PN has a quantum yield of $O_2(^1\Delta_g)$ generation close to unity. This quantum yield remains independent of solvent and this is the reason why PN may be established as a universal $O_2(^1\Delta_g)$ reference sensitizer [24].

From oxygen uptake, the initial slopes were determined in order to evaluate the rates of oxygen consumption by HSA, Andb and HSA-Andb.

2.2.3.2. Time-resolved phosphorescence detection of O_2 ($^1\Delta_g$) (TRPD)

The laser-kinetic spectrophotometer for time resolved phosphorescence detection of $O_2(^1\Delta_g)$ (TRPD) has been previously described [25]. Briefly, it consists of a Nd:YAG laser (Spectron) as the excitation source. The output at 355 nm was employed to excite the photosensitizer PN. The absorbance of the photosensitizer was 0.2-0.3 at the excitation wavelength. The kinetic decays of the phosphorescent signals were first order in all cases. The experiments were made in deuterated water, due to the enlargement of the $O_2(^1\Delta_g)$ lifetime in this solvent [26]. $O_2(^1\Delta_g)$ phosphorescence lifetimes were evaluated in absence (τ_0)

and in presence of different concentrations of Andb and/or HSA (τ). For the HSA-Andb system, the experiments were made at different Andb concentrations, while HSA concentration was kept constant. The overall rate constant for $O_2(^1\Delta_g)$ quenching, k_t (addition k_q + k_r, processes [4] and [5], respectively, in Scheme 1) were determined through Stern-Volmer treatment:

$$\frac{\tau_0}{\tau} = 1 + k_t \tau_0 [A] \qquad (7)$$

where [A] = molar concentration of Andb and/or HSA.

3. RESULTS AND DISCUSSION

The structures of Gli and Glip are shown in Fig. 1. pK_a values for Gli and Glip are 5.8 and 6.2, respectively [27]. Thus, both drugs may exist as ionized species under the experimental conditions (pH 7.4).

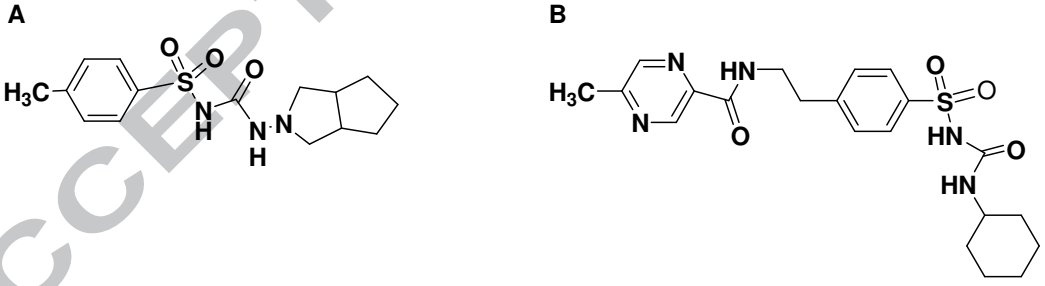

Fig. 1. Chemical structures of antidiabetic compounds: Gliclazide (A) and Glipizide (B).

Under the assumption that both Andb are weak acid compounds and could bind HSA, the binding between Gli or Glip and the protein was studied. In

this sense, the binding constants were evaluated and the number and identification of binding sites were determined.

3.1. Binding parameters

Solutions containing HSA ($1x10^{-5}$ M) were excited at 295 nm in order to ensure the exclusive excitation of residue Trp214. Changes in fluorescence intensities at 340 nm were determined in the presence of different concentrations of Andb. These data were processed, as previously described in section 2.2.1, in order to obtain $[Andb]_{free}$ and <r> values. Results for Gli and Glip indicated that the best binding isotherm fit was obtained when n=2 (Fig. 2). This means that both Andb could bind HSA in two sites. Thus, the correspondent binding constants K_{bi} and K_{bii} were determined from the fitting of the binding isotherm (Eq. 1).

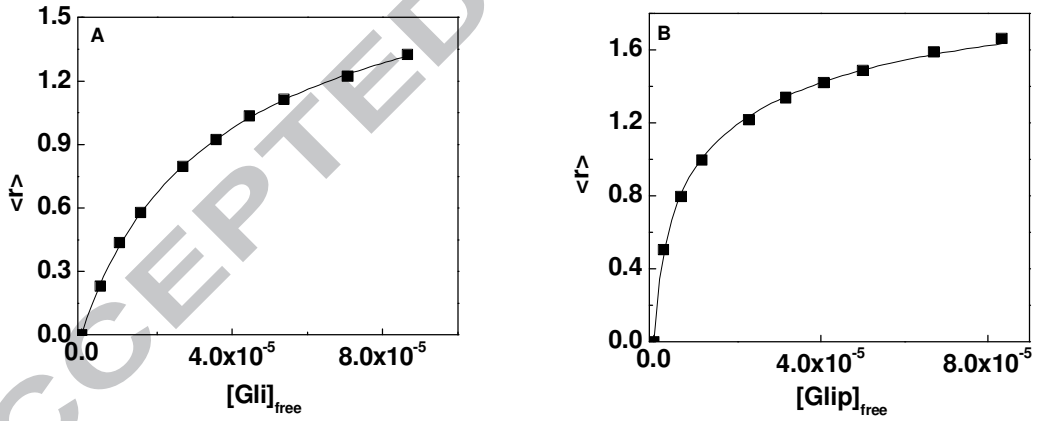

Fig. 2: Binding isotherm for Gli (A) and Glip (B) at 299.2 K and 299.6 K, respectively. <r> represents the binding density; $[Gli]_{free}$ and $[Glip]_{free}$ are the molar concentrations of Gli or Glip unbound to HSA.

The binding constants were determined at different temperatures in order to investigate the potential dependence between both variables (Eq. 5). Results are shown in Table 1. As can be observed, the binding constants K_{bi} and K_{bii} are the same order of magnitude for Gli, while K_{bi} values are higher than K_{bii} for Glip. Binding constants for Gli and Glip are in agreement with values (10^4–10^5 M^{-1}) reported for the interaction between HSA and other hypoglycemic compounds [28,29].

Table 1: Binding constants (K_{bi}) for HSA-Andb complexes obtained at different temperatures, in buffered solution at pH 7.4 (10% methanol). λ_{exc} = 295 nm; λ_{emi} = 340 nm.

Andb	temperature (K)	K_{bi} x10^4 (M^{-1})	K_{bii} x10^4 (M^{-1})
Gli	285	(4.9±0.2)	(1.15±0.06)
	292	(3.8±0.2)	(1.02±0.06)
	299	(4.4±0.2)	(1.28±0.05)
	308	(4.2±0.2)	(1.03±0.06)
Glip	285	(58±3)	(2.83±0.07)
	291	(46±3)	(2.8±0.1)
	299	(31±2)	(2.46±0.09)
	308	(29±1)	(2.32±0.07)

As can be seen, over the range of temperatures studied (285.6 K-308.5 K), the binding constants values for Gli did not change significantly with the temperature.

In the case of Glip, binding constants were found to decrease with increasing temperature (Table 1), indicating thereby that the interaction is exothermic.

From the variation of the binding constants with temperature observed for Glip, the thermodynamic parameters ΔH^0 and ΔS^0 were determined from Eq. 5. Through these values and the respective ΔG^0 values (Eq. 6), the nature of the protein-ligand association process can be explained. In this sense, a hypothetical thermodynamic model has been proposed, which occurs in two steps [30]. The first step represents a hydrophobic association and partial immobilization, and the second includes all other intermolecular interactions such as electrostatic, Van der Waals, H-bonds. The net ΔG^0 for the complete association process is essentially determined by the relative magnitude of ΔS^0 and ΔH^0 associated at each step. The values of thermodynamic parameters are shown in Table 2.

Table 2. Thermodynamic parameters obtained for the binding between HSA and Glip in buffered solutions at pH 7.4 (10% Methanol).

Site	ΔHº (Kcal/mol)	ΔSº (cal/mol K)	[a]ΔGº (Kcal/mol)
Site i	-5.4	7	-7.5
Site ii	-1.6	14.6	-5.9

[a] values were obtained at 299 K.

As presented in Table 2, for both binding sites negative ΔH^0 and positive ΔS^0 values were obtained. Thus, the resulting negative ΔG^0 values demonstrated that binding is a spontaneous process. High ΔH^0 values indicated that binding between HSA and Glip is an enthalpically controlled and favored process. As was proposed, negative ΔH^0 values may be related to van der

Waals or hydrogen bonding interactions [30]. In this sense, Glip is one of the sulfonylureas possessing higher hydrogen-bonding capacity (9 proton acceptor groups and 3 proton donor groups) and therefore hydrogen bonding may be the interactions involved in the HSA-Glip association process [27].

On the other hand, it can be suggested that net positive ΔS^0 values may be due to energetic contribution of the hydrophobic association, related to the first step that involves a reorganization of the solvent structure around the protein and the ligand [30]. The ΔS^0 sign could be explained in terms of a great disorder in the solvent structure around the protein-ligand complex as compared to the isolated hydrated species.

Regarding the binding parameters, it is important to notice that from the analysis of fluorescence data and the subsequent fit of binding isotherms, it is only possible to estimate the number of binding sites and to calculate the binding constants. However, it is not possible to assign each binding constant to a particular site. In order to support the experimental data based on the number of sites of interaction between HSA and Andb and to suggest the possible location of these sites, docking experiments were performed in this study.

3.3. Docking assays

The method used was validated by correlating the warfarin, diazepam and azapropazone positions after docking in binding sites I, II and III respectively, with the position of the same ligand in the crystal complexes 2BXD, 2BXF and 2BX8. Since the root mean square deviation (rmsd) between both structures (docked and crystal complex) was of 1.33 Å for warfarin, 0.86 Å for diazepam and 1.87 Å for azapropazone, the method was considered

reliable. As a first step, a search of pockets in the HSA with the IcmPocketFinder tool of ICM-Pro software with default parameters was performed. Three pockets were selected for docking studies. Two of them are the well-known sites I and II described by Sudlow [22]. The third one was selected after an analysis of binding capabilities of HSA, defined by crystallographic studies. For this, a search of all HSA molecules co-crystallized with ligands was carried out in Protein Data Bank. The superimposition of all these structures showed a region where several ligands were bound and it was coincident with a bulky pocket detected by icmPocketFinder. We called this site binding site III. A representation of the pockets is shown in Fig. 3.

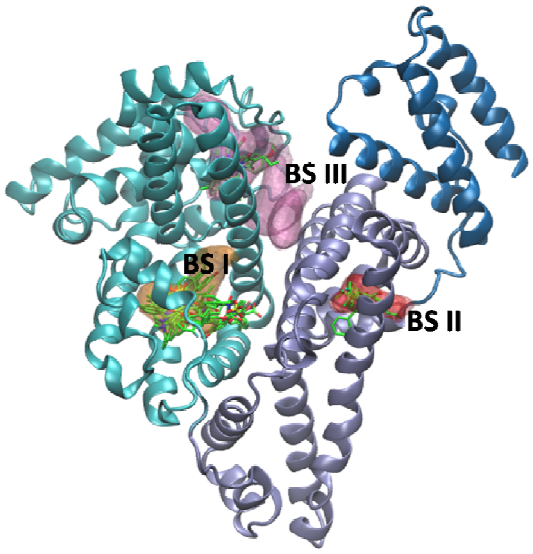

Fig. 3. Cartoon representation of HSA and the three cavities used in this study in a transparent mesh representation: Binding site I (BS I), binding site II (BS II) and binding site III (BS III). Ligands found in these cavities are represented in sticks (structures listed in section 2.2.2).

3.3.1. Docking in binding site I

The binding site I is located in subdomain IIA (Fig. 3), and it is formed by residues Tyr150, Glu153, Phe157, Glu188, Ala191, Ser192, Lys195, Gln196, Lys199, Phe211, Trp214, Ala215, Arg218, Leu219, Arg222, Phe223, Leu238, His242, Arg257, Leu260, Ala261, Ile264, Ser287, His288, Ile290, Ala291 and Glu292. The entrance to the pocket is formed by charged residues and the core, by hydrophobic side chains. Docking with ligands, Gli and Glip, while mapping this pocket resulted in conformations located outside the pocket in the cleft between domains I and III, and since the location was mostly in a region of solvent accessibility, the possibility of binding in this region was discarded.

3.3.2. Docking in binding site II

This binding site is located in subdomain IIIA (Fig. 3), which is smaller than site I and is formed by residues Leu387, Ile388, Gln390, Asn391, Phe403, Leu407, Arg410, Tyr411, Lys414, Leu430, Val433, Ala449, Leu453, Arg485, Ser489. In this case, there is predominance of positive electrostatic potential and a hydrophobic core in the pocket. Docking with Gli and Glip when mapping this site resulted in conformations occupying entirely the pocket. Fig. 4 shows the ligand site obtained for Gli (Fig. 4A) and for Glip (Fig. 4B) in solid and in transparent surface with residues in a 4 Å radius. In both cases, there is predominance of hydrophobic interactions with the methylpyrazide and perhydrociclopenta[c]pyrrole groups of Glip and Gli respectively. In the case of Gli, a cation-π interaction between Arg410 and the benzene ring of the ligand is also observed, with an average distance of 4.3 Å; and an H-bond between O3 of Gli and hydroxyl group of Ser489.

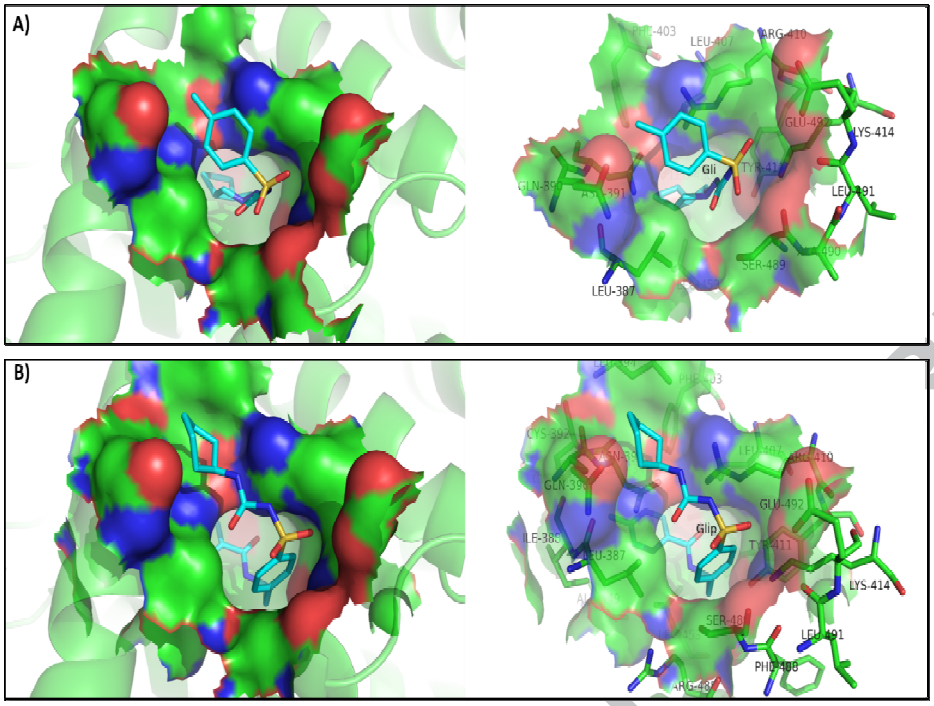

Fig. 4. Docking of Gli (A) and Glip (B) in site II: best conformations obtained are showed as sticks colored by atom type. Ligand site is represented as solid and transparent surface.

Binding energies obtained were favorable in both cases; for Gli -80.3 Kcal mol^{-1}, and for Glip -101 Kcal mol^{-1}. In the surroundings of the ligands, residues Lys410 and Tyr411 are located, and they have been noted as important in ligand binding. The obtained conformations are located in similar positions as ligands diazepam, 3-carboxy-4-methyl-5-propyl-2-furanpropionic, ibuprofen and 5-(2,4-difluorophenyl)-2-hydroxy-benzoic acid, present in crystallographic structures 2BXF, 2BXA, 2BXG, 2BXE, respectively.

3.3.3. Docking in binding site III

The binding site III is located in the subdomain IB and in the interphase with subdomain IIIA (Fig. 3) and is constituted by residues Asp108, Asn109,

Pro110, Leu112, Leu115, Val116, Arg117, Pro118, Met123, Phe134, Lys137, Tyr138, Glu141, Ile142, Arg145, His146, Pro147, Tyr148, Phe149, Tyr161, Leu182, Leu185, Arg186, Asp187, Gly189, Lys190, Ala191, Ser193, Ala194, Arg197, Glu425, Asn429, Lys432, Tyr452, Val456, Gln459, Val462 and Leu463. It is a very bulky pocket formed mainly by positively charged and hydrophobic residues. Docking mapping this site resulted in two major conformations for both ligands (Fig. 5 and 6).

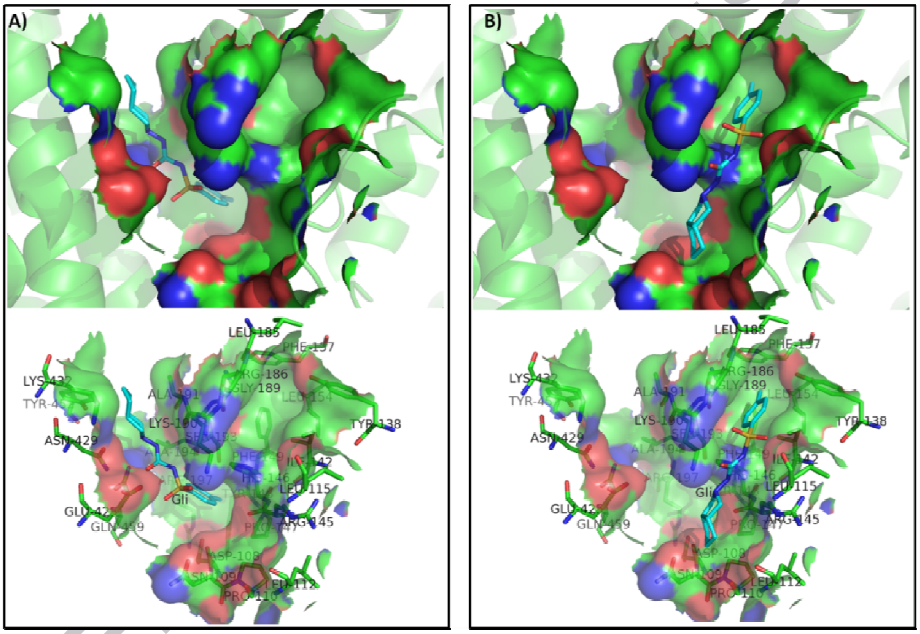

Fig. 5. Docking of Gli in site III: best conformation obtained is displayed in (A) and alternative conformation in (B). Gli is showed as sticks colored by atom type and ligand site are represented as solid and transparent surface.

For Gli (Fig. 5), the best conformation had a binding energy of -94.3 Kcal mol^{-1} (Fig. 5A). This conformer is stabilized principally by H-bonds. One of them, between sulfonyl group and the amino group of the Lys190 side chain; Other H-bonds could be established between the O3 and N1 of Gli with the side

chains of Glu425, Gln459, Asn429. It also seems to contribute to a π-π stacking interaction between His416 and the benzenic ring with an average distance of 4.6 Å between both rings. An alternative conformation was obtained with a binding energy of -86.5 Kcal mol^{-1} (Fig. 5B). This conformer is stabilized by two H-Bonds between O3 and N1 of Gli with the side chain of Lys190, and hydrophobic interactions around the benzenic ring. Despite the lower energy, this alternative conformation is located in a similar position as indomethacine and azapropazone ligands present in crystal structures 2BXQ, 2BXM, 2BX8 and 2BXI.

For Glip, binding energies of both conformations were similar: -122 Kcal mol^{-1} (Fig. 6A) and -120 Kcal mol^{-1} (Fig. 6B).

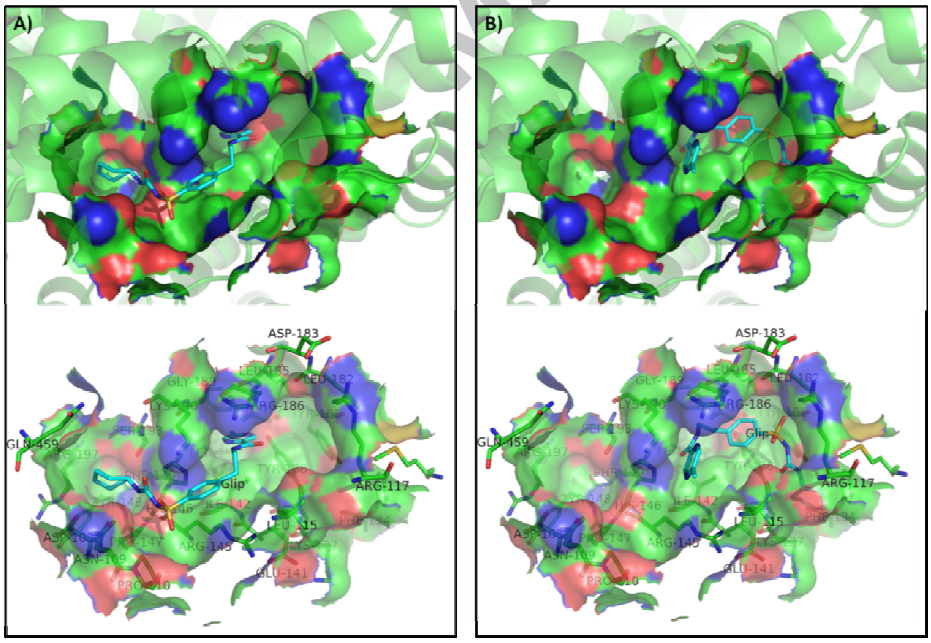

Fig. 6. Docking of Glip in binding site III: best conformation obtained is displayed in (A) and alternative conformation in (B). Glip is showed as sticks colored by atom type and ligand site are represented as solid and transparent surface.

The moiety of the molecule containing the methylpyrazide group is located in the same region of indomethacine and azapropazone ligands as observed for Gli, but the rest of the ligand molecule adopts in each conformation an opposite orientation in the cavity. The conformer 1 is stabilized by H-bonds between O1, N2, N2 and N5 of Glip and the side chains of residues Lys190, Arg145 and Tyr138. A cation-π interaction between the benzenic ring of Glip and the amino group of the side chain of Lys190 is also noted, with an average distance of 3.7 Å. In the conformer 2, the interactions observed are four H-bonds between O1, 0,3, N3 and O4 of Glip and side chains of residues Tyr161, Arg117, Arg186 and His146; and a cation-π between the methylpyrazide ring and the amino group of the side chain of residue Lys190 with an average distance of 4.1 Å.

In summary, docking results are consistent with the binding of two molecules of Gli or Glip, one, in binding site II, and the other in binding site III. These results are in agreement with previous reports since several drugs were reported as having the capacity to bind to more than one site in HSA, for example, indomethacine and azapropazone bind to binding sites I and III and ibuprofen binds to sites I and II [31].

On the other hand, conventional binding studies between several compounds and HSA have postulated the sites I and II as the only probably binding sites [32-34]. In the last decade, docking assays have demonstrated that there are other cavities distributed across the protein that act as alternative binding sites. Site III has been described as a preferred site for several drugs in other docking studies [35]. These authors suggest that the steric factor seems to play the most important role in the transportation of drugs by HSA.

3.4 Sensitized photoxidation of Andb and HSA

Results obtained from binding and docking experiments have demonstrated that Gli and Glip effectively interact with HSA. Therefore, the $O_2(^1\Delta_g)$-photodegradation of the free and Andb-bounded protein was investigated. Regarding the eventual interaction between HSA and the sensitizer PN, absorption spectra of PN (0.06 mM) as a function of HSA concentration (0-0.05 mM) were determinated. Due to the fact that these absorption spectra did not change (data not shown), the interaction between 0.01 mM HSA and 0.06 mM PN can be considered negligible.

The results presented in this section were interpreted and discussed following the processes shown in the next scheme.

$$S + h\nu \rightarrow {}^1S^* \xrightarrow{k_{isc}} {}^3S^* \qquad [1]$$

$${}^3S^* + O_2\,({}^3\Sigma_g^-) \xrightarrow{k_{ET}} S + O_2\,({}^1\Delta_g) \qquad [2]$$

$$O_2\,({}^1\Delta_g) \xrightarrow{k_d} O_2\,({}^3\Sigma_g^-) + \text{heat or } h\nu \qquad [3]$$

$$O_2\,({}^1\Delta_g) + A \xrightarrow{k_q} O_2\,({}^3\Sigma_g) + A \qquad [4]$$

$$O_2\,({}^1\Delta_g) + A \rightarrow AO_2 \xrightarrow{k_r} \text{products} \qquad [5]$$

Scheme 1. Photosensitized generation and deactivation processes of O_2 ($^1\Delta_g$). S: sensitizer (PN); A: photooxidable substrate (Andb, HSA); k_{isc}: intersystem crossing rate constant; k_{ET}: energy transfer rate constant; k_d: non radiative decay rate constant; k_q: physical deactivation rate constant; k_r: chemical deactivation rate constant.

Scheme 1 depicts a generic photosensitized process mediated by $O_2(^1\Delta_g)$. The absorption of incident light promotes the sensitizer S (PN) to its electronically excited singlet state ($^1S^*$) and subsequently, to its electronically excited triplet state ($^3S^*$) *via* intersystem crossing (process 1). An energy transfer process from $^3S^*$ to O_2 ($^3\Sigma_g^-$) (oxygen in its ground state) dissolved in the medium can yield $O_2(^1\Delta_g)$ (process 2), which can decay either by collision with surrounding solvent molecules (process 3), or by interaction with a photooxidizable substrate A (Andb or HSA) through physical and/or chemical processes (steps 4 and 5, respectively).

Photoirradiation at λ>320 nm of the system PN/Andb and/or HSA/ oxygen produced modifications in the absorption spectra of photooxidizable substrates, indicating chemical changes in the compounds. In parallel, oxygen uptake was observed (Fig. 7).

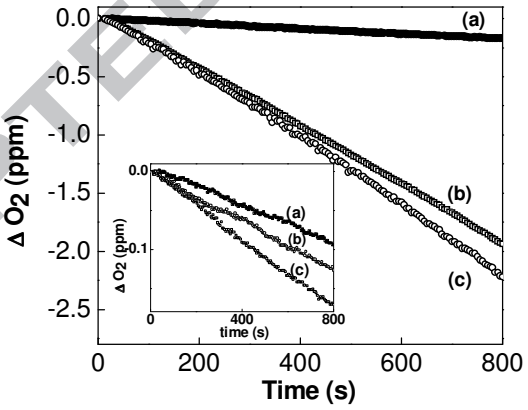

Fig. 7. Oxygen uptake as a function of photoirradiation time by buffered solutions at pH 7.4 (10% methanol) of PN ($Abs_{365\ nm}$= 0.5) in presence of: Main Figure: 0.5 mM HSA (a), 0.5mM Gli (b), 10 μM HSA: 0.5 mM Gli (c). Insert: 0.5

mM Glip (a), 10 μM HSA: 0.5 mM Glip (b), 0.5 mM HSA (c). Sensitizer: PN ($Abs_{365\ nm}$= 0.5).

From oxygen consumption plots, initial rates were determined as shown in Table 3, where they are expressed as relative oxygen uptake rates (v_r).

Table 3. Rate constant values for the overall quenching of $O_2(^1\Delta_g)$ (k_t) by HSA, HSA:Gli and HSA:Glip and relative rates of oxygen consumption (v_r) upon PN sensitization, in air-equilibrated buffered solutions at pH 7.4 (10% Methanol).

System	v_r	[a] k_t x10^{-7} ($M^{-1}s^{-1}$)
Gli	1.9	2.2
Gli-HSA	2.6	4.5
Glip	0.2	1.2
Glip-HSA	0.7	4.7
HSA	1.0	80

[a] Deuterated solutions were only employed in the determination of k_t values.

As can be seen in Table 3, Gli and the system HSA-Gli have higher reactivity than the protein. In the case of HSA-Gli, this increment may be interpreted in terms of additive contributions of each component. On the other hand, the system HSA-Glip has less reactivity than HSA, which could be interpreted as an auto-protective effect from the system as a whole, against photooxidative damage in respect to the protein. Furthermore, the results show that Gli is more photooxidizable than Glip against $O_2(^1\Delta_g)$.

The overall deactivation of $O_2(^1\Delta_g)$ by Andb, HSA and HSA-Andb was quantified from the overall rate constant k_t. Results are shown in Table 3. As can be noticed, k_t value for the protein indicated that HSA is a better $O_2(^1\Delta_g)$ deactivator than both Andb. By comparing k_t values for both HSA and HSA-Gli system, it can be observed that the binding of Gli to the protein exerts a protective effect on the system as a whole. On the assumption that the reactive component was the only contribution to the overall $O_2(^1\Delta_g)$-deactivation for Gli and HSA, it would be expected that k_t value for the system HSA-Gli were equal to the addition of individual contributions of each compound, as was observed for v_r values. However, the decrease on k_t values may be attributed to an additional effect, as a consequence of the binding between Andb and the protein. In this sense, it is well known that sensitized photooxidation in proteins involves aminoacids as cysteine, methionine, histidine, tryptophan, and tyrosine.[36] More specifically, Tyrosine residues are known to be good physical $O_2(^1\Delta_g)$ deactivators under neutral pH condition. Docking assays suggested that Gli and Glip bind in site II and site III and that several tyrosine residues are involved in these binding sites. In Fig. 4, the participation of Tyr411 in binding site II can be noticed. Likewise, when Gli binds to site III, the residue Tyr452 is involved in one conformation (Fig. 5A), and the residue Tyr138, in the other conformation (Fig. 5B). In the case of Glip, bound in site III, the participation of the residues Tyr161 and Tyr138 in both conformations can be seen (Fig. 6A and 6B). Therefore, the decrease observed in k_t values when the Andb are bound to the protein, compared to k_t value for HSA free, may be attributed to the reduction of the availability of Tyrosine residues which can physically deactivate the $O_2(^1\Delta_g)$.

4. CONCLUSIONS

We propose that antidiabetic compounds, Gli and Glip, binds to HSA on sites II and III, with binding constants values in the order of 10^4-10^5 M^{-1}. Thermodynamic parameters indicated that HSA-Glip interaction is an enthalpically controlled and favored process, governed by hydrogen bonding and hydrophobic interactions.

Oxygen uptake experiments strongly suggest that the system HSA-Glip experiments a sort of self-protection effect against photooxidative damage as compared to the isolated protein. It was also found that Glip is less photooxidizable than Gli by the species $O_2(^1\Delta_g)$. Furthermore, the binding between Andb and the protein generates a decrease in k_t values that may be explained in terms of a reduction in the number of tyrosine residues involved in the interaction, which have the capacity to physically deactivate $O_2(^1\Delta_g)$.

Acknowledgements

Financial support from Consejo Nacional de Investigaciones Científicas y Técnicas (CONICET) and Secretaría de Ciencia y Técnica de la Universidad Nacional de Río Cuarto (SECyT-UNRC) Argentina, is gratefully acknowledged. P.R. Beassoni, N.A. García, M.A. Biasutti and S. Criado are career members of CONICET. C. Challier thanks CONICET for a PhD fellowship, and C. Boetsch would like to acknowledge fellowship support from CONICET and the Ministerio de Ciencia y Tecnología- Córdoba (MinCyT-Cba). P.R. Beassoni thanks Dr. Danilo-Gonzalez Nilo from Centro de Biología Integrativa y Bioinformática de la Universidad Andres Bello, Chile for access to computational facility.

References

[1] Alberts, B., Johnson, A., Lewis, J., Raff, M., Roberts, K., and Walter, W. Molecular Biology of the Cell, 4th edition. Garland Science. New York. 2002.

[2] Roberts, J. A., Pea, F., Lipman, J. The clinical relevance of plasma protein binding changes. Clin Pharmacokinet (2013) 52:1–8.

[3] Roche, M., Rondeau, P., Singh, N. R., Tarnues, E., Bourdon, E. The antioxidant properties of serum albumin. Febs Letters (2008) 582:1783-1787.

[4] Diagnosis and classification of diabetes mellitus. Diabetes Care. (2010). 33:S62-S69.

[5] Brownlee, M. Negative consequences of glycation. Metab.Clin. Exp. (2000). 49:9-13.

[6] Gribble, F.M., Riemann, F. Sulphonylurea action revisited: the post-cloning era. Diabetologia (2003) 46:875–891.

[7] Griffith Hardman, J., Limbird, L. E., Gilman, A. G. Las bases farmacológicas de la terapéutica. Goodman & Gilman. 9th edition. McGraw-Hill / Interamericana de España, S.A. Madrid. (2001)

[8] Baynes J.W. Role of oxidative stress in development of complications in diabetes. Diabetes (1991). 40:405-412.

[9] Nishikawa, T., Edelstein, D., Du, X.L., Yamagishi, S., Matsumura, T., Kaneda, Y., Yorek, M.A., Beebe, D., Oates, P. J., Hammes, H.P., Giardino, I., Brownlee, M. Normalizing mitochondrial superoxide production blocks three pathways of hyperglycaemic damage. Nature. (2000). 404:787-790.

[10] Tiedge, M., Lortz, S., Drinkgern, J., Lenzen, S. Relation between antioxidant enzyme gene expression and antioxidative defense status of insulin-producing cells. Diabetes. (1997). 46: 1733–1742.

[11] Maechler, P., Jornot, L., Wollheim, C. B. Hydrogen peroxide alters mitochondrial activation and insulin secretion in pancreatic beta cells. J. Biol. Chem. (1999).274: 27905–27913.

[12] Sirotkin, V.A., Borisover, M.D., Solomonov, B.N. Effect of chain length on interactions of aliphatic alcohols with suspended human serum albumin. Binphys. Chem. (1997). 69:239-248.

[13] Kragh-Hansen, U., Chuang, V.T.G., Otagiri, M., Practical aspects of the ligand-binding and enzymatic properties of human serum albumin. Biol. Pharm.Bull (2002). 25:695-704.

[14] Groemping, Y., Hellmann, N. Spectroscopic Methods for the Determination of Protein Interactions. Curr. Protoc. Protein Sci. (2005).39:20.8,1–27.

[15] Klotzt, I.M., Hunston, D.L. Properties of graphical representations of multiple classes of binding sites. Biochemistry. (1971).10:3065-3069.

[16] Stinson, R., Holbrook, J.J. Equilibrium binding of nicofinamide nucleotides to lactate dehydrogenases. J. Biochem. (1973). 1319:719-728.

[17] Ward, L.D. Measurement of ligand binding to proteins by fluorescence spectroscopy. Methods Enzymol. (1985) 117:400-414.

[18] Origin (OriginLab, Northampton, MA).

[19] Beassoni, P; Otero, LH; Boetsch, C; Domenech, CE; González-Nilo, FD and Lisa, AT. Site-directed mutations and kinetic studies show key residues involved in alkylammonium interactions and reveal two sites for phosphorylcholine in Pseudomonas aeruginosa phosphorylcholine phosphatase. Biochim. Biophis. Acta. (2011). 1814:858-863.

[20] Abagyan, R.; Trotov, M; Kuznetsov, D. A new method for structure modeling and design: applications to docking and structure prediction from the distorted native conformation. J. Comput.Chem. (1994).15:488–506.

[21] http://pubchem.ncbi.nlm.nih.gov/

[22]Sudlow G., Birkett D. J., Wade D. N.The characterization of two specific drug binding sites on human serum albumin. Mol. Pharmacol. (1975). 11:824-832.

[23] Bertolotti S. G., Arguello G. A., García, N. A. Effect of the peptide bond on the singlet molecular oxygen mediated photooxidation of tyrosine and tryptophan dipeptides. A kinetic study. J. Photoch. Photobio.B (1991). 10:57-70.

[24] Schweitzer, C., Schmidt, R. Physical mechanisms of generation and deactivation of singlet oxygen. Chem. Rev. (2003), 103:1685-1757.

[25] Miskoski, S., Bertolotti, S., Arguello, G., Garcia, N.A. On the $O_2(^1\Delta_g)$-mediated photooxidative behaviour of tripeptideglycyltyrosyl-alanine in alkaline medium: a kinetic study. Amino Acids (1993) 4:101–103.

[26] Nonell, S.L, Moncayo, F., Trull, F., Amat-Guerri, F., Lissi, E., Soltermann, A.T., Criado, S., Garcia, N.A. Solvent influence on the kinetics of the photodynamic degradation of Trolox, a water-soluble model compound for vitamin E. J. Photoch. Photobiol., B. (1995). 29:157-162.

[27] Remko, M. Theoretical study of molecular structure, pKa, lipophilicity, solubility, absorption, and polar surface area of some hypoglycemic agents. J. Mol. Struct. Theochem. (2009) 897:73–82.

[28] Seedher, N., Kanojia, M. Mechanism of interaction of hypoglycemic agents glimepiride and glipizide with human serum albumin. Cent.Eur. J. Chem. (2009). 7:96-104.

[29] Seedher, N., Kanojia, M. Reversible binding of antidiabetic drugs, repaglinide and gliclazide, with human serum albumin. Chem. Biol. Drug Des (2008). 72:290–296.

[30] Ross, P.D., Subramanian, S. Thermodynamics of protein Association. Biochemistry. (1981). 20:3096-3102.

[31] Ghuman, J., Zunszain, P. A., Petitpas, I., Bhattacharya, A. A., Otagiri, M., Curry, S. Structural basis of the drug-binding specificity of human serum albumin. J. Mol. Biol. (2005). 353:38–52.

[32] Sevilla, P., José M. Rivas J. M., García-Blanco, F., García-Ramos J.V., Sánchez-Cortés S. Identification of the antitumoral drug emodin binding sites in bovine serum albumin by spectroscopic methods. Biochim. Biophys. Acta. (2007). 1774:1359–1369.

[33] Tushar K. M., Kalyan, S. G., Anirban, S., Swagata,D. The interaction of silibinin with human serum albumin: A spectroscopic investigation. J. of Photochem. Photobiol. A: Chemistry (2008). 194:297–307.

[34] Seedher, N., Bhatia, S. Reversible binding of celecoxib and valdecoxib with human serum albumin using fluorescence spectroscopic technique. Pharmacol. Res. (2006) 54:77–84.

[35] Keshavarz, F., Alavianmher,M.M., Yousefi, R. Molecular dynamics simulation and docking studies on the binding properties of several anticancer drugs to human serum albumin. Mol. Biol. Res. Comm. (2012).1:65-73.

[36] Davies, M.J. Singlet oxygen-mediated damage to proteins and its consequences. Biochem. Biophys. Res. Comm. (2003). 305:761–770.

7-Respect to comments in point 7, notice that ΔS values are expressed in **cal**/molK, while ΔH values are expressed in **Kcal**/mol. Therefore, enthalpy values are predominant when compared with entropy values in the Van´t Hoff equation.

In the other hand, we have explained in page 14 that binding constants for Gli-HSA complex did not change over the range of temperature studied. In consequence, we are not allowed to determinate the thermodynamic parameters for this interaction. In case of Glip-HSA interaction, we did observed a variation in binding constant with temperature and therefore, we could determinate the thermodynamic parameters for the Glip-HSA association process.

Highlights

- Fluorescence and docking assays showed that Gli and Glip bind to HSA on two sites
- The interaction between HSA and Glip is a favored, enthalpically-controlled process
- Glip is less photooxidizable than Gli through a $O_2(^1\Delta_g)$-mediated process
- The HSA-Andb binding cause a decrease in the overall rate constant for $O_2(^1\Delta_g)$ quenching